In Situ, Time-Resolved X-ray Diffraction Study of the Solid-State Polymerization of Disulfur Dinitride to Poly(sulfur nitride)

H. Müller,* S. O. Svensson, J. Birch, and Å. Kvick

European Synchrotron Radiation Facility, B.P. 220, F-38043 Grenoble, France

Received September 18, 1996[⊗]

Products and kinetic and mechanistic aspects of the title reaction were investigated by time-resolved X-ray powder diffraction combined with Rietveld refinement. The polymerization of S_2N_2 at 40 °C was monitored with a time resolution better than one diffraction pattern per minute until completion. The reaction product comprised a mixture of monoclinic β-$(SN)_x$ (90%) and an additional orthorhombic phase, identified as α-$(SN)_x$ (about 10%). The inversely proportional conversion/formation vs time curves for educt and products indicate that the reaction involves only crystalline phases. The cell parameters of polymerizing S_2N_2 varied noticeably with progressing conversion, whereas the cell volume remained unchanged up to a monomer conversion of 50%. Refinement of atomic coordinates for S and N indicated retention of the reactant geometry. It is concluded that the polymerization of S_2N_2 to $(SN)_x$ is of nondiffusive nature and involves a martensitic transition.

Introduction

Poly(sulfur nitride), $(SN)_x$, is unique among polymeric materials: $(SN)_x$ represents a genuine, anisotropic conductor which exhibits a metal-like temperature dependence of the electrical resistivity and shows a superconducting transition at low temperature ($T_c \leq 0.3$ K).[1] The compound is usually obtained by spontaneous, thermally induced solid-state polymerization of disulfur dinitride, S_2N_2.[2,3]

Owing to its unprecedented and yet unmatched physical properties, $(SN)_x$ has been the focus of extensive studies, the major part of which aimed at a better understanding and improvement of its physical properties.[4] A reaction mechanism for the title reaction, based on the structures of the monomer, a partially polymerized S_2N_2 single crystal, and the product, has been proposed.[5]

Peculiarities of the $S_2N_2/(SN)_x$ system, however, such as the potential explosion hazard associated with the monomer as well as its instability and moisture sensitivity, limited *in situ* studies of the polymerization $S_2N_2 \rightarrow (SN)_x$ to spectroscopic methods, such as FT-IR spectroscopy.[6]

X-ray powder diffraction (XRD) combined with Rietveld analysis is a powerful tool for time-resolved studies of phase transformations and solid-state reactions. The advent of new, third generation synchrotron radiation sources such as the European Synchrotron Radiation Facility opened new areas for time-resolved X-ray diffraction experiments. High flux of well-collimated X-ray photons combined with fast read-out detectors allow time-resolved experiments even for poorly scattering samples. In the following we present the first *in situ* study of the solid-state polymerization of S_2N_2 to $(SN)_x$ monitored by X-ray powder diffraction. Kinetic and mechanistic aspects of the title reaction will be discussed and qualitatively compared to presently available theoretical considerations.

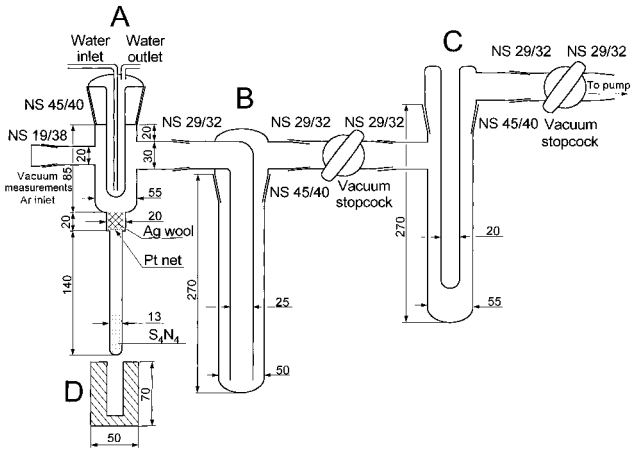

Figure 1. Apparatus for pyrolysis of S_4N_4 and subsequent sublimation of S_2N_2.

Experimental Section

Apparatus. The apparatus shown in Figure 1 was entirely constructed from Pyrex glass and attached to a double-stage mechanical pump (end pressure: 5×10^{-4} bar). Pressure in the system was monitored by a Pirani vacuum gauge. Infrared spectra were recorded with a Bruker IFS 28 FT-IR spectrometer using KBr disks.

X-ray Measurements. Data collection was performed at the Materials Science beamline of the European Synchrotron Radiation Facility.[7] Data were recorded with a monochromatized X-ray beam set to an energy of 38 keV. The beam size at the sample position was adjusted to 0.5×0.5 mm^2. The capillaries containing the monomer were mounted on a κ-diffractometer with a horizontal ϕ-axis. An X-ray image intensifier was used as detector system.[8] Data presented in this work were collected with exposure times of 2 and 20 s, during which the sample was spun by 10 and 45°, respectively. The diffraction images were corrected for inherent distortions of the detection system, beam decay, and background before Rietveld refinement. The diffraction patterns were refined with the Rietveld method using the program GSAS.[9] For all diffraction profiles the scale factors for S_2N_2 and $(SN)_x$

[⊗] Abstract published in *Advance ACS Abstracts,* March 1, 1997.

(1) Greene, R. L.; Street, G. B. *Phys. Rev. Lett.* **1975**, *34*, 577.
(2) Goehring, M.; Vogt, D. *Z. Allg. Anorg. Chem.* **1956**, *285*, 181.
(3) Mikulski, G. M.; Russo, P. J.; Saran, M. S.; Diarmid, A. G. M.; Garito, A. F.; Heeger, A. J. *J. Am. Chem. Soc.* **1975**, *97*, 6358.
(4) Street, G. B.; Greene, R. L. *IBM J. Res. Dev.* **1977**, 99.
(5) Baughman, R. H.; Chance, R. R. *J. Chem. Phys.* **1976**, *64*, 1869.
(6) Kanazawa, H.; Stejny, J.; Keller, A. *J. Mater. Sci.* **1990**, *25*, 3838.
(7) Krumrey, M.; Kvick, A.; Schwegle, W. *Rev. Sci. Instrum.* **1995**, *66*, 1715.
(8) Moy, J. P. *Nucl. Instrum. Methods* **1994**, *A348*, 641.
(9) Larson, A. C.; von Dreele, R. B. *Los Alamos Laboratory Rep.* **1987**, LA-UR-86-748.

S0020-1669(96)01141-X CCC: $14.00

were refined by employing structural parameters taken from the literature.[3,10] Further details of measurement and data treatment are described elsewhere.[11]

Reagents. Silver wool (Aldrich) was opened and stored under an Ar atmosphere. Tetrasulfur tetranitride was prepared from SCl_2 and ammonia according to the literature procedure,[2,12] purified by recrystallization from benzene, and dried *in vacuo*. The compound was checked by elemental analysis, TLC (silica/CCl_4; $R_f = 0.5$), and its infrared spectrum[13] and used without further purification.

Method. In a typical experiment, S_4N_4 (0.5 g; 5.42 mmol) was placed at the bottom of reaction tube A as indicated in Figure 1. To prevent any S_4N_4 from sticking to the walls, a long-stemmed funnel was used for loading. Then, platinum mesh was placed at the bottom of the cove of A. Silver wool (500 mg) was thoroughly packed onto the platinum mesh support. A thermocouple was attached by means of a heating wire to the outside glass surface of the cove and secured with metal hose bands. A second thermocouple was attached in an identical fashion to the outer surface of copper cylinder D. D was placed underneath A and lifted horizontally with the help of a lab-jack until the bottom of A touched the bottom of the cylindrical bore of D. The apparatus was evacuated to 10^{-3} bar and then cold trap B was immersed into a dewar filled with liquid nitrogen, cold trap C being at ambient temperature. The upper heating wire was turned on; after D warmed to 300 °C, the temperature was adjusted to 80 °C.

As soon as D had reached a temperature of 60 °C, pressure increased to around 8 10^{-3} bar, indicating the onset of sublimation. After the S_4N_4 vapors had been pumped for 30−45 min through the wool, a blue film started to appear on the inlet tube of cold-trap B; a similar film started to form on the outer glass surface of the water-cooled finger of reaction tube A. After the pyrolysis products had collected on the inlet tube of trap B for 5 h, heating was stopped. At that stage the water-cooled finger of A was covered with a golden film of $(SN)_x$ and the inlet of cold trap B was covered with yellow, red, and blueish deposits, whereas the lower part of the inlet tube of cold trap B was coated by a white film of S_2N_2 (below the liquid N_2 level). Cold trap C was then immersed in a dewar filled with liquid nitrogen, and the temperature of cold trap B was raised to around 0 °C by an ice-water bath. Around 30 min after the start of the second sublimation a white film became visible on the uppermost part of trap C. Around 4 h after the start of the second sublimation, the cooling baths were removed, and the whole apparatus was filled with dry Ar (99.999%) via a gas-inlet valve attached to A by means of a stainless steel cone with flange. After pressure equalization, monitored by a safety valve (bubbler), the two vacuum stopcocks on either side of cold trap C were closed to separate trap C from the rest of the setup. Immediately after the vacuum was broken, the inner cooling finger of cold trap C was filled with finely crushed dry ice. With both stopcocks closed, trap C, containing the S_2N_2, was transferred with permanent cooling (−78 °C; dry ice) to a glovebag. The glovebag was evacuated and refilled five times with high-purity nitrogen (99.9999%). Finally the inner and outer parts of cold trap C were separated, and S_2N_2 was removed with a small spatula, ground in an agate mortar, and filled into glass capillaries (i.d. 0.8 mm). The capillaries were sealed with plasticine, taken out of the glovebag, flame sealed, and stored in liquid nitrogen under exclusion of light until the start of the measurements.

With regard to the well-known explosion hazards connected with the handling of S_4N_4, and particularly S_2N_2, we note that throughout a whole series of runs (15 experiments) we did not encounter any problems. However, during the sealing of the capillaries two violent detonations occurred. Taking into account the tiny masses handled (1−3 mg per capillary), appropriate safety measures (use of protective shield) through preparation/handling of S_4N_4 and S_2N_2 are strongly recommended.

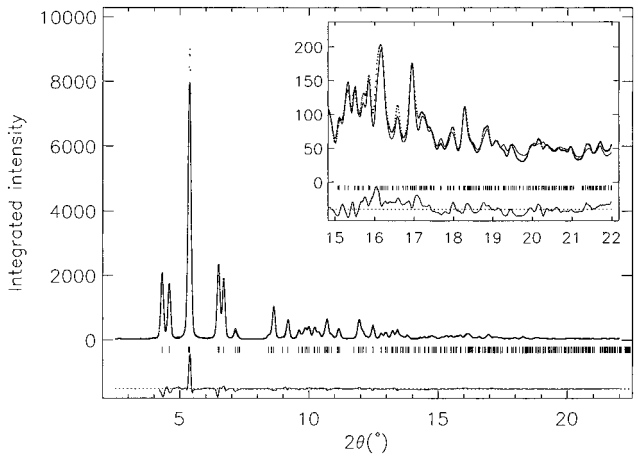

Figure 2. Diffraction pattern of S_2N_2 before reaction onset ($t = -2000$ s). Dotted line: observed pattern. Solid line: calculated pattern. Solid line (bottom): difference curve.

Results and Discussion

Educt and Products. A typical diffraction pattern of the starting compound S_2N_2 is displayed in Figure 2. Cell and refinement parameters are summarized in Table 1. Experimental data and calculated profiles for S_2N_2 are in good accordance, albeit the unit cell parameters slightly deviate from the previously reported values. Literature data refer to a structure elucidation at −130 °C,[3] whereas the cell parameters of S_2N_2 in the present work were determined at room temperature ($T = 20 \pm 1$ °C). The contents of the most likely crystalline impurities in the monomer, $(SN)_x$ and S_4N_4, amounted to less than 0.1% each, from results of the Rietveld refinement.

Microcrystalline S_2N_2 in sealed capillaries turned out to be remarkably stable at ambient temperature. Though the aspect of the powder changed from off-white to blue, diffraction patterns did not noticeably alter within 60 min. Therefore, polymerization was accelerated by radiation heating with a halogen lamp which raised the sample temperature from 20 to 40 °C within 60 s. The possibility of the light-induced generation (300 nm $\leq \lambda \leq$ 550 nm) of $(SN)_x$ has been reported; however, photoinitiation was only successful at the solvent/crystal interface and failed for S_2N_2 crystals without mother liquor.[14] Accordingly, polymerization in the present case is a *thermally* initiated rather than a *light*-initiated process.

At the end of the diffraction experiments ($t \gg 6000$ s), the capillaries contained a black powder which exhibited a golden-metallic luster. A micrograph of the crystalline, polymeric product, as recovered after breaking of a glass capillary, is displayed in Figure 3. The grain size distribution of the samples typically ranged from 1 to 10 μm. The crystallites show the striated surfaces characteristic of $(SN)_x$, a consequence of the fibrillar nature of the polymer. Infrared absorptions of the reaction product at 1002, 698, 670, 620, and 510 cm^{-1} are consistent with bands reported in previous work.[3,13,15] The observed diffraction pattern of the polymerization product and the calculated diffractogram of β-$(SN)_x$ are displayed in Figure 4; cell and refinement parameters are given in Table 1. The unit cell parameters of the polymer agree well with results of XRD and neutron scattering studies,[3,16] which employed β-$(SN)_x$ formed by *thermal* solid-state polymerization of S_2N_2, and thus corroborate the presumption of a thermally induced process in

(10) Cohen, M. J.; Garito, A. F.; Heeger, A. J.; MacDiarmid, A. G.; Mikulski, G. M.; Saran, M. S.; Kleppinger, J. *J. Am. Chem. Soc.* **1976**, *98*, 3844.
(11) Svensson, S. O.; Birch, J.; Müller, H.; Kvick, Å. *J. Synchrotron Rad.*, in press.
(12) Villena-Blanco, M.; Jolly, W. L. *Inorg. Synth.* **1967**, *9*, 1967.
(13) Macklin, J. W.; Street, G. B.; Gill, W. D. *J. Chem. Phys.* **1979**, *70*, 2425.
(14) Love, P.; Kao, H. I. ; Labes, M. M. *J. Chem. Soc., Chem. Commun.* **1978**, 301.
(15) Kanazawa, H.; Stejny, J.; Keller, A. *J. Mater. Sci.* **1991**, *26*, 1635.
(16) Heger, G.; Klein, S.; Pintschovius, L.; Kahlert, H. *J. Sol. State Chem.* **1978**, *23*, 341.

Table 1. Cell and Refinement Parameters

	compound				
	S_2N_2[a]	β-$(SN)_x$[b]	S_2N_2[c]	β-$(SN)_x$[d]	β-$(SN)_x$[e]
exposure time (s)			20	20	
structure	monoclinic	monoclinic	monoclinic	monoclinic	monoclinic
space group	$P2_1/c$	$P2_1/c$	$P2_1/c$	$P2_1/c$	$P2_1/c$[f]
a (Å)	4.485(2)	4.153(6)	4.518(1)	4.148(2)	4.431
b (Å)	3.767(1)	4.439(5)	3.845(1)	4.431(2)	4.148
c (Å)	8.452(3)	7.637(12)	8.495(1)	7.664(4)	7.383
β (deg)	106.43(3)	109.7(1)	106.43(1)	109.35(3)	α: 77.77
S1−N1 (Å)	1.657(1)	1.593(5)	1.659(5)		
S1−N2 (Å)	1.651(1)	1.628(7)	1.636(4)		
angle S−N−S (deg)	90.42(6)	119.9(4)	90.1(3)		
angle N−S−N (deg)	89.58(6)	106.2(2)	89.9(3)		
sulfur					
x	0.20243(8)	0.1790(8)	0.1994(3)		0.2127
y	0.1210(1)	0.7873(6)	0.1166(4)		0.0847
z	0.10635(4)	0.3443(4)	0.1054(2)		0.0943
U_{iso} (Å^2)			0.043(1)	0.038(2)	
nitrogen					
x	−0.1735(3)	0.141(3)	−0.175(1)		0.568
y	0.0475(4)	0.431(2)	0.0496(8)		0.069
z	0.0778(2)	0.322(2)	0.0751(3)		0.072
U_{iso} (Å^2)			0.043(1)	0.022(3)	
no. of params			21	15	
no. of data points			1728	1728	
R_p[g]			0.067	0.135	
wR_p[g]			0.078	0.176	
reduced χ^2			7.5	59	

[a,b] Structural values for S_2N_2 and β-$(SN)_x$ published by Cohen and co-workers.[10] The values for S_2N_2 were obtained at −130 °C. [c] Results of Rietveld refinement of diffraction pattern of S_2N_2 before reaction onset ($t = -2000$ s). [d] Results of Rietveld refinement of the diffraction pattern of β-$(SN)_x$ at the end of the reaction ($t = 6000$ s). [e] Structural parameters of β-$(SN)_x$ corresponding to Figures 8 and 12. Observe that α < 90°. Unit cell parameters were calculated with values from the column marked with footnote *d*, and atomic coordinates were from data from the column marked with footnote *b*.[10] [f] Symmetry operations are (x, y, z), $(x + {}^1/_2, -y, -z)$, $(-x, -y + {}^1/_2, -z + {}^1/_2)$, $(-x + {}^1/_2, y + {}^1/_2, z + {}^1/_2)$. [g] Definitions: $R_p = \sum|I_o - I_c|/\sum I_o$; w$R_p = [\sum w(I_o - SI_c)^2/\sum w(I_o)^2]^{1/2}$, where I_o is the observed intensity, I_c is the calculated intensity, w is the scale factor for each 2θ measurement, and S is the overall scale factor.[9]

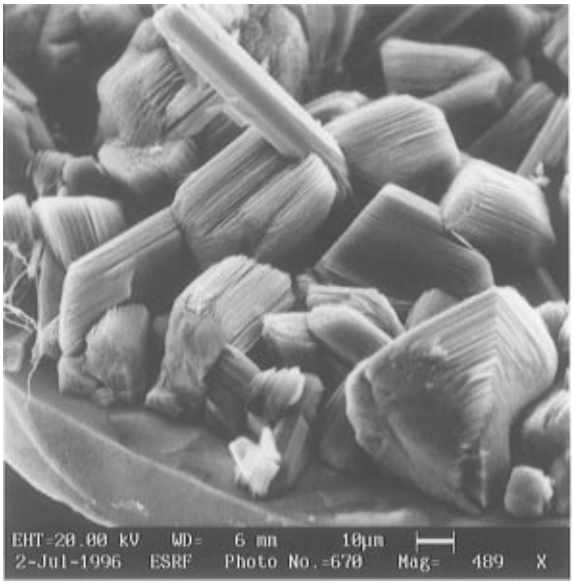

Figure 3. Micrograph of $(SN)_x$ crystals as found in the capillaries used for the measurements after completion of the reaction ($t \gg 6000$ s).

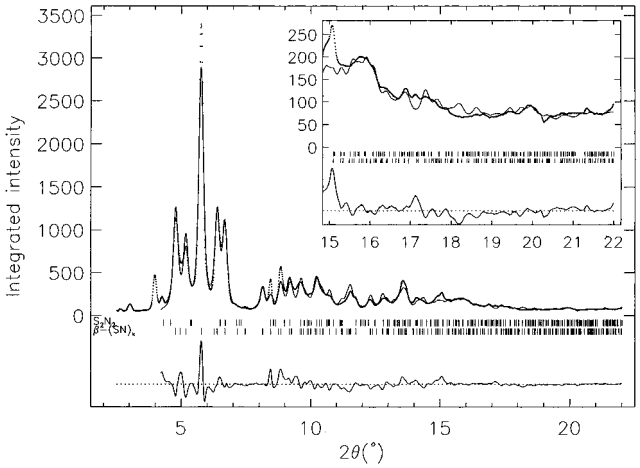

Figure 4. Diffraction pattern of $(SN)_x$ at the end of the reaction ($t = 6000$ s). Dotted line: observed pattern. Solid line: calculated pattern. Solid line (bottom): difference curve.

the present case. The monomer content at the end of the reaction was below the detection limit.

Three reflections in the range $2.5 \le 2\theta \le 4.5°$, not attributable to β-$(SN)_x$, made probable the presence of either S_4N_4 or an orthorhombic $(SN)_x$ phase with the unit cell parameters $a = 6.200$ Å, $b = 4.412$ Å, and $c = 4.709$ Å (space group $P222$). A comparison of experimentally observed and modeled diffraction peaks for S_4N_4 and α-$(SN)_x$ in this region is given in Figure 5. The good match of the calculated peak positions of α-$(SN)_x$ with the experimental profile certainly favors an assignment of the reflections in question to the presence of another $(SN)_x$ phase rather than to S_4N_4. The formation of orthorhombic α-$(SN)_x$ besides monoclinic β-$(SN)_x$ in the course of the title reaction could explain earlier observations concerning unassignable reflections in polymerization products of S_2N_2.[17] This view is further supported by the well-known and theoretically interpreted lack of structural perfection in β-$(SN)_x$ as expressed in the presence of fractionally occupied chain sites.[3,5,16,18] A correlation between these defect sites and the presence of a polytypic product mixture comprising α- and β-$(SN)_x$ is likely.[17]

(17) Baughman, R. H.; Apgar, P. A.; Chance, R. R.; MacDiarmid, A. G.; Garito, A. G. *J. Chem. Phys.* **1977**, *66*, 401.

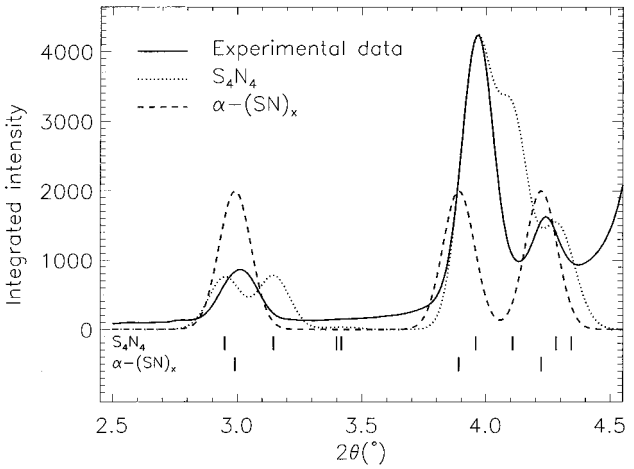

Figure 5. Comparison of observed peaks (solid line) and modeled peaks for S_4N_4 (dotted line) and α-$(SN)_x$ (broken line) in the range $2.5° \leq 2\theta \leq 4.5°$. The intensities for α-$(SN)_x$ are chosen arbitrarily. The vertical bars indicate the center of predicted peak positions.

The role of an orthorhombic, intermediate phase in the conversion from monomeric S_2N_2 to polymeric $(SN)_x$ has been discussed,[17,18] particularly with regard to the fact that β-$(SN)_x$ can (partially) be transformed into the α-phase by a shear transformation. Grinding of crystalline β-$(SN)_x$ yielded a mixture of β-$(SN)_x$ and a new, orthorhombic $(SN)_x$ phase (hereafter denoted as α-$(SN)_x$), as identified by X-ray powder diffraction and Weissenberg photographs,[17] which however was never obtained phase-pure. It is conceivable to presume that highly disordered but structurally closely related α-$(SN)_x$ cocrystallizes with the more regular β-phase.

Questions as to nature and composition of the polymerization product(s) of S_2N_2 dependent on the reaction conditions have been addressed in a number of publications.[2,19,20] To date, at least five different phases of $(SN)_x$ have been described, among which the β-phase generally is referred to as $(SN)_x$. Polymerization of S_2N_2 in dry air yielded $(SN)_x$, whereas reaction in ambient (humid) air gave a complex product mixture, comprising $(SN)_x$ (70%) and S_4N_4 (30%).[2] More recent work,[21] concerned with the influence of water on the polymerization process and the purity of the resulting $(SN)_x$, demonstrated the detrimental effects of water on both polymerization process and polymer. Though S_2N_2 itself behaved remarkably inert, the presence of water during polymerization led to the formation of unidentified compounds comprising N−H and S═O groups besides $(SN)_x$; the formation of S_4N_4 was not observed. The moisture sensitivity of the system $S_2N_2/(SN)_x$ has further been shown by mass spectroscopic studies: samples of "analytically pure" $(SN)_x$ contained hydride impurities possibly originating in residual water films on the glass surfaces of reaction vessels used for $S_2N_2/(SN)_x$ preparation.[19] Little is known about the other phases of $(SN)_x$. Electron diffraction studies provided evidence for the co-existence of at least one other monoclinic phase (denoted as α′) besides β-$(SN)_x$ which is believed to eventually transform after annealing into β-$(SN)_x$.[22] A correspondence of α′-$(SN)_x$ and α-$(SN)_x$ appears to be unlikely with regard to cell parameters and space groups but cannot be ruled out with certainty. A variety of substrate-dependent morphologies was observed during epitaxial polymerization of $(SN)_x$.[20]

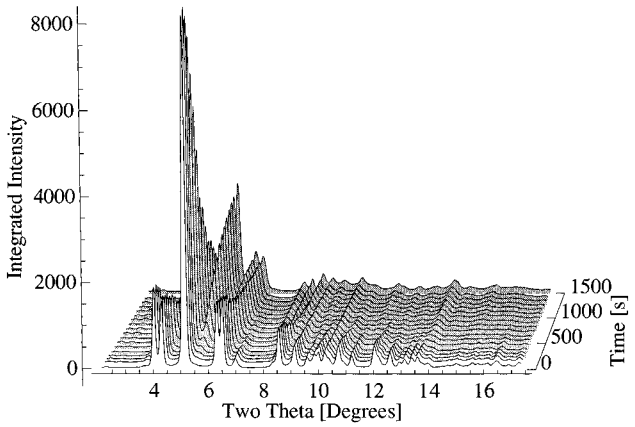

Figure 6. Diffraction patterns as a function of time recorded during the polymerization $S_2N_2 \rightarrow (SN)_x$ ($0 \leq t \leq 1500$ s). For clarity only every second collected pattern has been included.

Kinetic Aspects. The time-dependent evolution of diffraction patterns during the polymerization $S_2N_2 \rightarrow (SN)_x$ is shown in Figure 6. For clarity only every second collected pattern has been included. The origin of the time scale ($t = 0$) was set to the time when the reaction was started by irradiation with visible light; the range displayed covers the interval $0 \leq t \leq 1500$ s.

The conversion-time/formation-time curves for S_2N_2 and β-$(SN)_x$ were independently obtained from scale factors after refinement and are displayed in Figure 7a. Weights are given as mass percentages and are normalized with respect to the initial monomer mass (mass of S_2N_2 at $t = -2000$ s = 100%). The structure of α-$(SN)_x$ is unknown and consequently precluded any attempt to accurately determine its content in the reaction mixture. As can be read from Figure 7a, the product comprised after completion of the polymerization around 90% β-$(SN)_x$. It appears to be reasonable to assign the residual, weighted scattering intensity to α-$(SN)_x$. Values of 0% ($t = 0$) and 10% ($t = 6000$ s) were used for scaling the corresponding formation vs time curve (cf. Figure 7b).

The conversion/formation vs time curves for S_2N_2 and β-$(SN)_x$ exhibit characteristic, sigmoidal shapes which resemble that of autocatalytic polymerization processes.[23] The two graphs are approximately inversely proportional to each other; the formation of α-$(SN)_x$ follows a closely related time dependence. Restated in other words, the sum of the scale factors of S_2N_2 and both $(SN)_x$ phases amounts to almost 100% and is constant during the entire conversion. Therefore, the presence of an intermediate, non-, or partially crystalline phase which yields the final polymer after subsequent recrystallization, as presumed in earlier work,[5,18] appears to be very unlikely, unless recrystallisation kinetics were much faster than the time resolution of our measurements. Obviously, crystalline S_2N_2 directly converts into crystalline β-$(SN)_x$ and α-$(SN)_x$. Thus, provided the above conclusions are correct, diffusion processes are of little, if any, importance to the title reaction.

The slope of the S_2N_2 conversion curve corresponds to the reaction rate $r = -\mathrm{d}[S_2N_2]/\mathrm{d}t$ and deviates from zero only at $t \geq 200$ s. It seems reasonable to attribute the interval ($0 \text{ s} \leq t \leq 200$ s) to an induction period prior to the actual reaction. After the induction period, r increases considerably, as visualized by the steeply increasing slopes of conversion/formation curves ($200 \text{ s} \leq t \leq 500$ s). A 50% monomer conversion were

(18) Baughman, R. H.; Chance, R. R. *J. Polymer Sci. Pol. Phys. Ed.* **1976**, *14*, 2019.
(19) Smith, R. D.; Wyatt, J. R.; Weber, D. C. ; DeCorpo, J. J.; Saalfeld, F. E. *Inorg. Chem.* **1978**, *17*, 1639.
(20) Rickert, S. C.; Ishida, H.; Lando, J. B.; Koenig, J. L.; Baer, E. *J. Appl. Phys.* **1980**, *51*, 518.
(21) Ishida, H.; Rickert, S. C.; Hopfinger, A. J.; Lando, J. B.; Baer, E. *J. Appl. Phys.* **1980**, 5188.
(22) Boudeulle, M. Thesis, Lyon, France, 1974.
(23) Chance, R. R.; Patel, G. N. *J. Polymer Sci. Pol. Phys. Ed.* **1978**, *16*, 859.

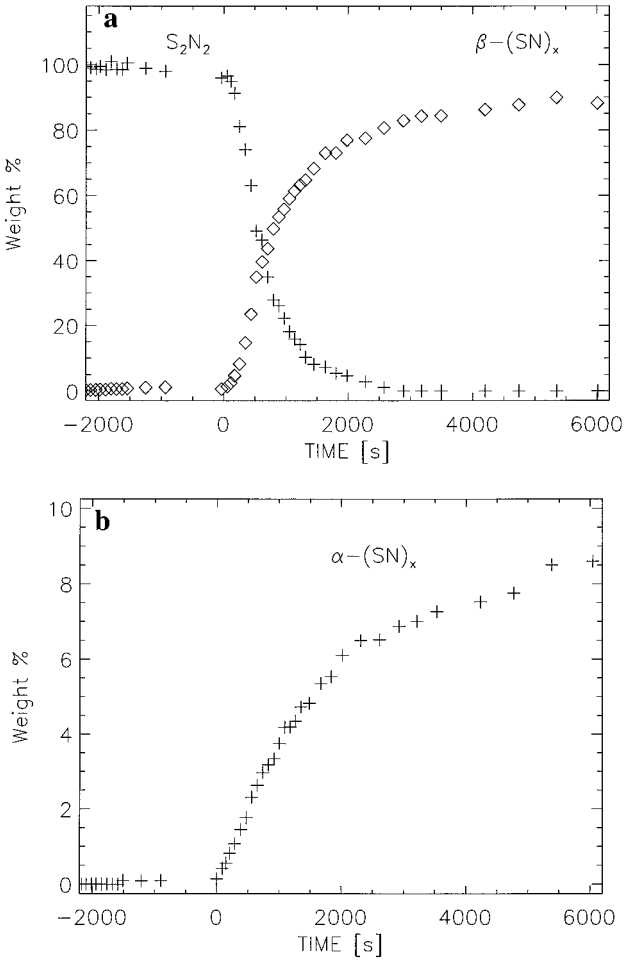

Figure 7. (a) Conversion vs time curve for S_2N_2 and formation vs time curve for β-$(SN)_x$. (b) Formation vs time curve for α-$(SN)_x$.

achieved within 500 s after the reaction onset; approximately 70% of the initial S_2N_2 had vanished after 1000 s. At $t > 500$ s, r gradually decreases to eventually approach a steady state region at $t > 3000$ s, indicating complete consumption of the monomer. The same general trend is also reflected in the graph corresponding to the formation of α-$(SN)_x$. The steep increase of its formation rate after reaction onset plausibly links its generation to the polymerization process. The sigmoidal shape of the conversion curve for S_2N_2 qualitatively accords with the results of time-resolved FT-IR studies,[6] albeit the time resolution achieved in the present work is much higher. The total conversion time (end point of reaction defined by the slope of the S_2N_2 conversion curve equal to zero) for sample masses on the order of 1−2 mg amounted to around 3500 s.

Time-resolved FT-IR spectroscopy gave conversion times of about 5 h for a thin film of S_2N_2 at 22 °C and of around 20 min at 40 °C , and induction periods amounted to 40 and 2 min, respectively.[6] ESR measurements of the radical concentration in polymerizing, microcrystalline thin films of S_2N_2 at ambient temperature showed that the radicals decayed in about 12 h, indicating the end of the reaction.[10] The observed difference in conversion times at elevated temperature could simply be the consequence of methodological restrictions: the increasing reflectance inferred by the metallic character of $(SN)_x$ films toward the end of polymerization could severely have hampered monitoring of weak absorption bands by IR spectroscopy and consequently have frustrated the accurate determination of the reaction end point. A strong dependance of reaction times on

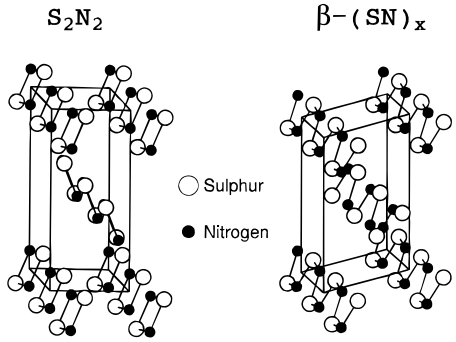

Figure 8. Crystal structures of S_2N_2 and β-$(SN)_x$.

crystal sizes has earlier been noticed and led to the assumption that the surface to volume ratio strongly influences reaction times.[15]

Mechanistic Aspects. Chemical reasoning as well as theoretical considerations led to the proposition that polymerization of S_2N_2 proceeds along the crystallographic a axis.[5,10] Initial ring opening of one S−N bond of adjacent S_2N_2 molecules was presumed to result in the formation of intermediate, short-lived S_2N_2 radicals.[10] Linear arrays of cleaved S_2N_2 molecules could thus recombine with little distortion of the molecular planes to directly yield covalently bond $(SN)_x$ polymer chains with the observed cis−trans configuration. The almost ideal square-planar S_2N_2 units form a typical herring-bone pattern and are aligned in alternatingly tilted rows along the a axis. Intermolecular S−N distances in pristine S_2N_2 (2.89 Å at −130 °C) are well below the sum of the corresponding van der Waals radii (3.4 Å),[3] indicative of a considerable intermolecular interaction. To facilitate further discussion, Figure 8 shows the crystal structures of S_2N_2 and $(SN)_x$, respectively, with the same axes notation chosen for both. The presentation of the $(SN)_x$ unit cell is unusual in that the crystallographic a and b axis were interchanged. The advantage of the chosen unit cells lies in the fact that the visualization of the spatial orientation of S_2N_2 molecular planes relative to $(SN)_x$ chains is much easier than for any orthodox notation. The resulting unit cell parameters are given in Table 1. For an equivalent, albeit more conventional, structure presentation the reader is kindly requested to refer to the original literature.[3]

As readily recognizable, the unit cell of S_2N_2 has to undergo a considerable distortion during the polymerization process. Since the unit cell parameters of S_2N_2 and $(SN)_x$ differ, the title reaction involves a shortening of a (0.087 Å; 1.9%) and c (1.112 Å; 13.1%), as well as an expansion of b (0.303 Å; 7.9%). Furthermore, the S_2N_2 angles α and β decrease from their initial values of 90° and 106.43° to 77.77 and 90° in β-$(SN)_x$, respectively. The cell volume of the educt is about 7% smaller than that of the product.

Alterations of both cell parameters and atomic positions could be monitored for the first 500 s of the polymerization reaction, a time interval corresponding to 50% monomer conversion. As depicted in Figure 9, the onset of the conversion ($t = 0$) is accompanied by an immediate and pronounced elongation of the cell axes of S_2N_2. The relative length changes amount to around 0.1% in the a and c directions and to about 0.05% difference for b. For the angle β the effect is less marked but still visible. The sharp discontinuities are caused by the rapid temperature increase from 20 to 40 °C and reflect the anisotropic thermal expansion of S_2N_2. It is worth noticing that these temperature-dependent variations correspond well to the observed differences of S_2N_2 cell parameters at −130 °C and room temperature. For the same reason, it is not possible to directly compare cell parameters resulting from a structure determination

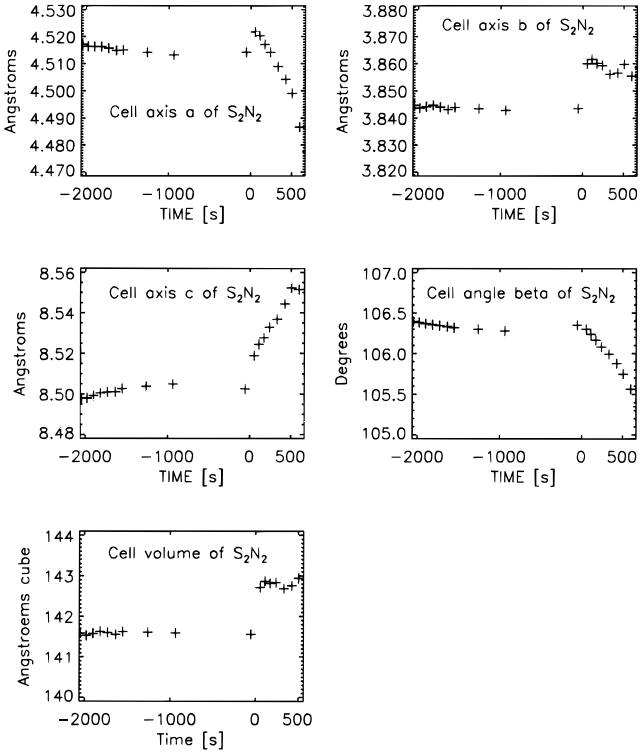

Figure 9. Variations of unit cell parameters $a-c$, angle β, and unit cell volume of S_2N_2 with time ($0 \leq t \leq 1000$ s).

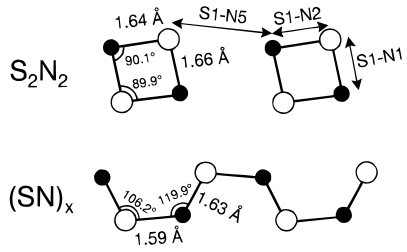

Figure 10. Intramolecular bond distances and angles of S_2N_2 ($t = -2000$ s; parameters from this work) and β-$(SN)_x$ (parameters from Cohen et al. [10]), both projected onto the 010 plane.

of a partially polymerized S_2N_2 crystal at −130 °C with the data of this work.[10]

With progressing monomer conversion ($t \leq 500$ s), the *a* axis and the angle β shrank in a nearly linear fashion by about 1% and *c* expanded by around 0.5%, whereas *b* and the cell volume remained virtually constant. Compared to thermal dilatation, these variations are small and suggest that the initial molecular arrangement of the reactant remains intact.

The unprecedented possibility to refine atomic positions of polymerizing S_2N_2 up to 50% conversion permitted one to obtain information regarding time-dependent rearrangements on a molecular scale. The experimental accuracy for the determination of atomic positions, however, is less reliable than the standard deviations for the unit cell parameters and thus restricts conclusions to qualitative trends.

After reaction onset, the intramolecular bond lengths S1−N2 and S1−N1 increased from about 1.65 Å ($t = 0$) to around 1.66 Å ($t = 500$ s). The bond angles remained constant (90°), so that within experimental accuracy the square-planar molecule geometry was retained. Simultaneously the intermolecular distances S1−N5 slightly shortened from 2.92 to 2.89 Å (cf. Figures 10 and 11), a feature consistent with the observed contraction of *a*. In this context, it should be recalled that the energy gap between ground and excited states of S_2N_2 is in the order of *kT* at room temperature and thus in principal allowed

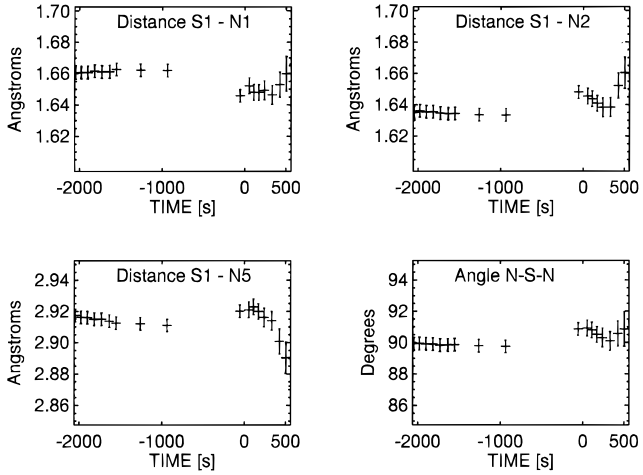

Figure 11. (a) Variation of intramolecular bond distance S1−N1 of S_2N_2 with time ($-2000 \leq t \leq 500$ s). (b) Variation of intramolecular bond distance S1−N2 of S_2N_2 with time ($-2000 \leq t \leq 500$ s). (c) Variation of intermolecular bond distance S1−N5 of adjacent S_2N_2 with time ($-2000 \leq t \leq 500$ s). (d) Variation of bond angle N−S−N of S_2N_2 with time ($-2000 \leq t \leq 500$ s). For the definitions of S1, N1, etc., see Figure 10. The indicated error bars correspond to $\pm\sigma$, where σ is estimated from standard deviations of cell parameters and atomic positions after refinement.

for a more than marginal population of excited levels.[24−27] *Ab initio* calculations, performed for intermediate, excited singlet, and triplet states of S_2N_2, predicted an increase of bond lengths to 1.69 Å with preservation of geometry for the former, whereas the latter should result in a rhombohedral distortion of the reactant molecules with significantly increased bond lengths (1.81 Å).[24] The observed alterations of intramolecular bond lenghts, however, do not easily lend themselves to conclusions regarding the occupancy of thermally excited states, whereas the shortening of intermolecular distances during the polymerization points to an important role of S−N contacts between adjacent reactant molecules.

Polymerization of S_2N_2 under hydrostatic pressure showed indeed that crystal strain as result of a mismatch between monomer/polymer lattice dimensions is not of significance for polymerization kinetics,[15] thus emphasizing the importance of nearest-neighbor interactions for the kinetics of the title reaction. As manifested in the fibrillar nature of the polymer, long-range coherence during polymerization is to be found only along *a*, but not in transverse directions, an obvious consequence of short intermolecular contacts in that orientation.

The variation of cell parameters *and* the constancy of the cell volume up to conversions as high as 75%, as observed in this work, could indicate that the polymer enters the polymerizing lattice as a solid solution[5] and, hence, support presumptions that the title reaction occurs as a single-phase polymerization.[6] Such an interpretation, however, contradicts the experimental finding that throughout the reaction only crystalline educt and product phases are involved. Furthermore, the retention of the reactant geometry up to high conversion levels is difficult to rationalize, unless one assumes that monomer and polymer in polymerizing S_2N_2 crystals are separated by a phase boundary. Consequently, any polymerization mechanism requiring diffusion processes, as implied by the postulated formation of a solid solution of monomer and polymer, appears to be unlikely.[5,18]

(24) Palmer, M. H.; Findlay, R. H. *J. Mol. Struct.* **1983**, *92*, 373.
(25) Salahub, D. R.; Messmer, R. P. *J. Chem. Phys.* **1976**, *64*, 2039.
(26) Salahub, D. R.; Messmer, R. P. *Phys. Rev. B* **1976**, *14*, 2592.
(27) Yamabe, T.; Tanaka, K.; Fukui, K.; Kato, H. *J. Phys. Chem.* **1977**, *81*, 727.

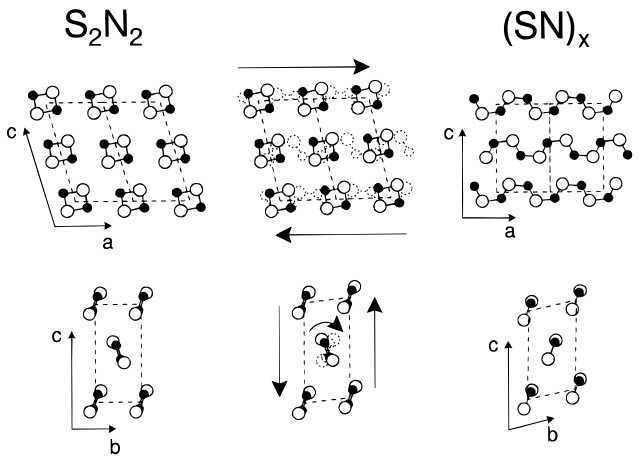

Figure 12. Schematic representation of rearrangements resulting from simultaneous shears parallel to the 001 plane (top) and parallel to the 010 plane (bottom). For further explanations, see the text.

It has been proposed[18] to interprete the title reaction as a lattice shear parallel to the 001 planes of S_2N_2 combined with a contraction of the *ab* plane and local atomic rearrangements which bring the sheared parent phase into correspondence with the daughter phase. As schematically visualized in Figure 12, such a geometric shear of S_2N_2 results indeed in a molecular rearrangement which resembles the actual structure of β-$(SN)_x$. It should be recalled, however, that the molecular planes of S_2N_2 are approximately parallel to the crystallographic 011 and $01\bar{1}$ planes, respectively, whereas all $(SN)_x$ chains are aligned in exactly the same fashion (parallel to the $01\bar{1}$ plane). Thus, a simple shear parallel to the 001 plane does not necessarily cause a rotation of the middle row of S_2N_2 molecules by 45° about the *a* axis, as indicated in Figure 12. A second, simultaneous shear component parallel to the 010 plane is required to achieve the molecular orientation observed in the final product (cf. Figure 12). Following this line of reasoning, only a separation of the postulated shear into a shear component parallel to the interface (habit) 001 plane and a dilatation component normal to the interface plane, i.e. parallel to the 010 plane, results in a shape *and* a volume change,[28] respectively, as required when going from S_2N_2 to β-$(SN)_x$. Schematically, the geometric transformation is accompanied by a contraction of the interplanar distances from 8.495 to 7.215 Å; the latter value matches quite well with the actual length of *c* (7.383 Å) in β-$(SN)_x$, as shown in Figure 8. Hence, the title reaction could be described as martensitic transition,[28] during which S_2N_2 closely approaches the molecular arrangement of $(SN)_x$ followed by ring cleavage and subsequent polymerization of the resulting radical intermediates. It should be emphasized that major rearrangements of the S_2N_2 structure are accomplished during the shear process prior to bond-breaking; consequently subsequent ring-opening of S_2N_2 and polymer formation require only minor atomic displacements.

This view is in full accordance with least-motion calculations[5] and completes and partially corrects a previously proposed polymerization mechanism.[10] Obviously, only a diffusionless nature of the polymerization, an inherent feature of martensitic transitions, is compatible with the observed conversion characteristics as well as with the retention of reactant geometry. Furthermore, the involvement of such type of phase transition casually explains the complicate structural changes needed for the formation of the $(SN)_x$ lattice.[10] The required symmetry preservation during the solid-state reaction and the statistically equal probability to break either the "upper" or "lower" S−N bond of S_2N_2 (cf Figure 10) result in the well-defined defect structure of β-$(SN)_x$ and could also account for the formation of α-$(SN)_x$ and its co-existence with β-$(SN)_x$.

Supporting Information Available: Listings of observed and calculated intensities *I*(obs) and *I*(calc) of S_2N_2 and $(SN)_x$ as obtained from Rietveld refinement (39 pages). Ordering information is given on any current masthead page.

IC961141Y

(28) *Treatise on Solid State Chemistry*; Hannay, N., Ed.; Plenum Press: New York, London, 1975; Vol. 5.